

## Oxidation state of the lithospheric mantle beneath Diavik Diamond Mines, Central Slave Craton, Canada

Steven Creighton<sup>1</sup>, Thomas Stachel<sup>1</sup>, David Eichenberg<sup>2</sup>, Robert W. Luth<sup>1</sup>

<sup>1</sup>Department of Earth and Atmospheric Sciences, University of Alberta, Edmonton, Canada

<sup>2</sup>Diavik Diamond Mines Inc., Yellowknife, Canada

We have studied the major and trace element chemistry of 31 garnet peridotitic xenoliths from the A154-North and South kimberlite pipes at Diavik Diamond Mines, in northern Canada. Eighteen of the samples have coarse or granuloblastic textures and the remaining 14 have porphyroclastic or mosaic porphyroclastic textures.

We measured the chemical composition of coexisting minerals, touching where possible, using electron probe microanalysis. Trace element concentrations of garnets were measured *in situ* using LA-ICPMS. Additionally, we used the newly developed flank method (Höfer and Brey 2007), incorporating the modifications of Creighton et al. (2008), for measuring the ferric iron concentration of garnet in our samples. As an electron microprobe technique, the flank method has the advantage of being an *in situ* technique with very high spatial resolution (>30×30 μm). The accuracy of ferric iron measurements made with the flank method is comparable to Mössbauer spectroscopy but the flank method has greater precision (Figure 1).

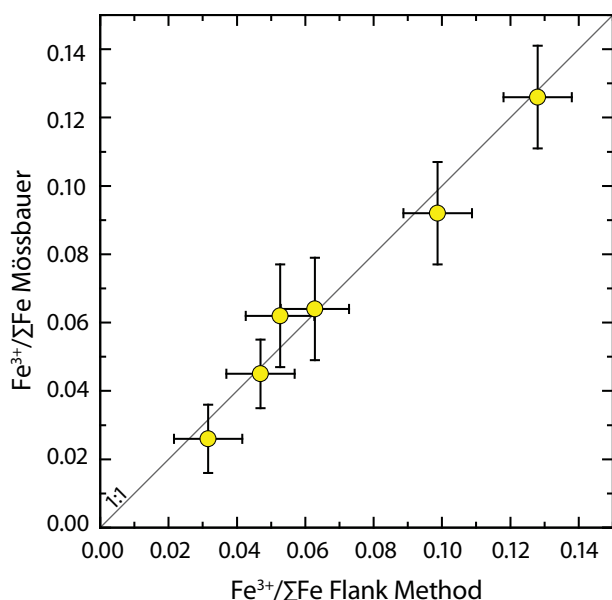


Figure 1: Comparison of  $\text{Fe}^{3+}/[\text{Fe}^{3+}+\text{Fe}^{2+}]$  in garnets measured using an electron microprobe (flank method) and a Mössbauer milliprobe.

### Mineral Chemical Data

Our analytical data on the major and minor element chemistry of xenolith minerals are similar to previous studies on garnet peridotites from the central Slave

Craton (Pearson et al. 1999; Menzies et al. 2004; Aulbach et al. 2007). For 30 of our samples, garnets are lherzolitic in composition, 12 classify as high-Ti peridotitic (G11, see Grütter et al. (2004)) and one classifies as G1, with low  $\text{Cr}_2\text{O}_3$  and high  $\text{TiO}_2$  concentrations similar to megacryst garnets. Based on garnet composition, only one the xenoliths classifies as harzburgitic (containing G10D garnet, Figure 2). Olivine and orthopyroxene are magnesian with molar Mg-Numbers ( $100 \times [\text{Mg}/(\text{Mg}+\text{Fe})]$ ) ranging from 89.7 to 93.0 and 88.5 to 93.9, respectively. Chrome diopside is observed in 27 of our 31 samples.

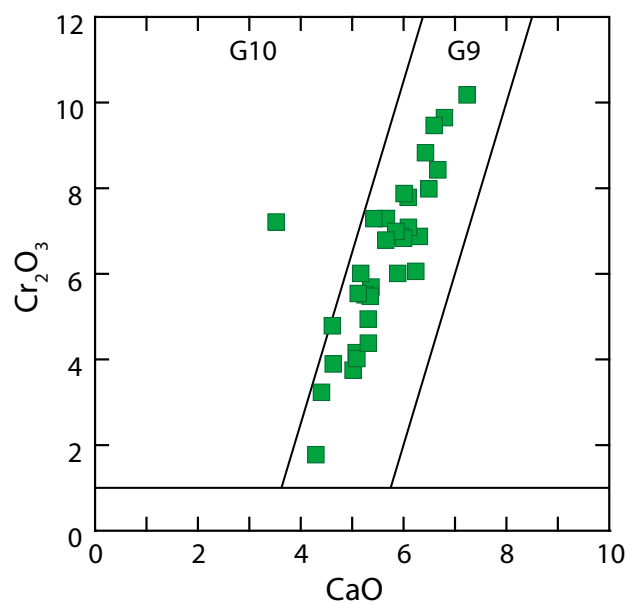


Figure 2: Composition and classification of garnets from xenoliths included in this study. Compositional fields are from Grütter et al. (2004).

Temperatures and pressures of latest equilibration were calculated using the olivine-garnet Fe-Mg exchange thermometer (O'Neill and Wood 1979) in combination with the Al-in-orthopyroxene barometer of Brey et al. (1990). The calculated temperatures and pressures range from 715 to 1210°C and 2.6 to 5.8 GPa, respectively. Samples from our xenolith suite predominantly plot between 40 and 42 mW/m<sup>2</sup> model geotherms, irrespective of texture. There is a "kimberlite sampling gap", with none of our xenoliths being derived from pressures between ~3.25 and 4.5 GPa, equivalent to approximately 95 to 140 km depth.

There are four types of chondrite normalized rare earth element (REE<sub>N</sub>) patterns observed in garnets from our samples (Figure 3a, b). Six garnets have sinusoidal REE<sub>N</sub> patterns – positive slopes to a maximum at Sm<sub>N</sub> followed by negative slopes to a trough at Ho<sub>N</sub> and 4-7× chondritic Lu (red circles in Fig. 3a). Garnets from 13 samples have normal patterns – steep positive slopes from LREE<sub>N</sub> to MREE<sub>N</sub> and flat slopes at approximately 10-20× chondritic concentration through MREE and HREE (purple hexes in Fig. 3a). Three garnets with normal REE<sub>N</sub> patterns have super-chondritic La concentrations and negative slopes from La<sub>N</sub> to Ce<sub>N</sub>. Seven garnets are moderately sinusoidal – steep positive slopes through the LREE<sub>N</sub> to a maximum at Sm<sub>N</sub> then negative slopes to Tm<sub>N</sub> or Yb<sub>N</sub>, followed by a positive slope to 5-8× chondritic Lu (green stars in Fig. 3b). The remaining five garnets have u-shaped patterns - LREE concentrations from 1-10× chondritic followed by a negative slope to a trough through the MREE<sub>N</sub> and positive slopes to Lu at 2-8× chondritic concentration (blue squares in Fig. 3b). Garnets with u-shaped REE<sub>N</sub> patterns are only observed in xenoliths from <110 km depth whereas garnets with normal patterns occur in xenoliths from depths >140 km, consistent with the lithospheric mantle beneath the Slave craton being divided into an “ultradepleted” (predominantly harzburgitic) shallow layer and a more fertile (predominantly lherzolitic) deeper layer (Griffin et al. 1999).

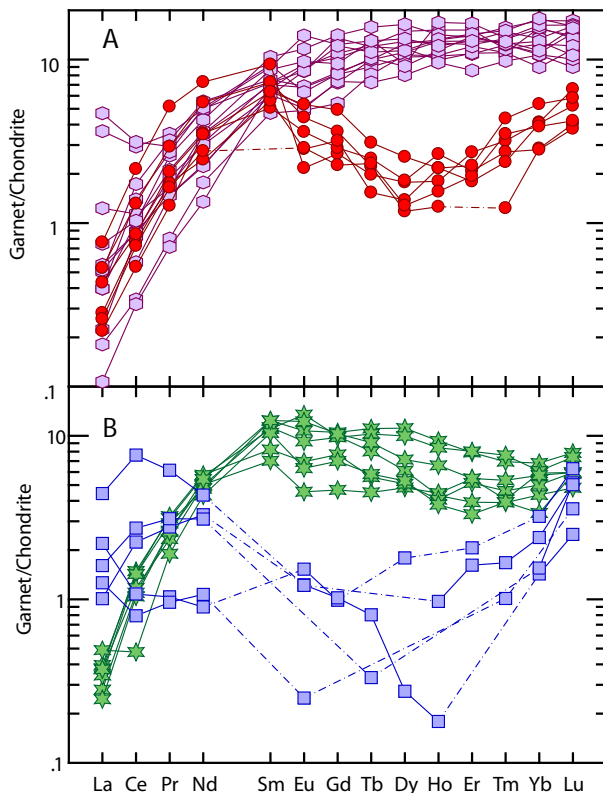


Figure 3. Chondrite-normalized REE patterns of xenolith garnets. Dashed lines link analyses skipping elements below the detection limit and are not intended to represent implied concentrations.

### Oxygen Fugacity

We calculated the oxygen fugacity of our samples, expressed relative to the FMQ buffer ( $\Delta \log fO_2$  (FMQ)), using the experimental calibration of the garnet peridotite oxybarometer of Gudmundsson and Wood (1995). The  $\Delta \log fO_2$  (FMQ) of our samples ranges over four orders of magnitude from 0.95 to -3.75 and, overall, our samples are more oxidized than other sections of subcratonic mantle previously measured.

According to thermochemical constraints, the garnet-bearing lithospheric mantle should become progressively more reduced with increasing pressure and temperature. Samples with evidence for the least degree of metasomatic re-enrichment (i.e. xenoliths with garnets having u-shaped REE<sub>N</sub> patterns) may be viewed as only very mildly metasomatized protolith of xenoliths with garnets having sinusoidal or normal REE<sub>N</sub> patterns. Thus, the “pre-metasomatic” redox profile for the central Slave Craton can be defined by the depth- $fO_2$  co-variation predicted for an isochemical increase in pressure and temperature along a 41 mW/m<sup>2</sup> model geotherm starting at the P-T- $fO_2$  conditions of the most depleted xenoliths derived from the shallower ultradepleted layer (shaded area in Figure 4). The deeper, more fertile xenoliths are more reducing than the predicted redox profile (Figure 4). This observation implies that the re-fertilization of the deeper portions of the central Slave lithospheric mantle was driven by ascending reducing melts and fluids promoting diamond formation and stabilization.

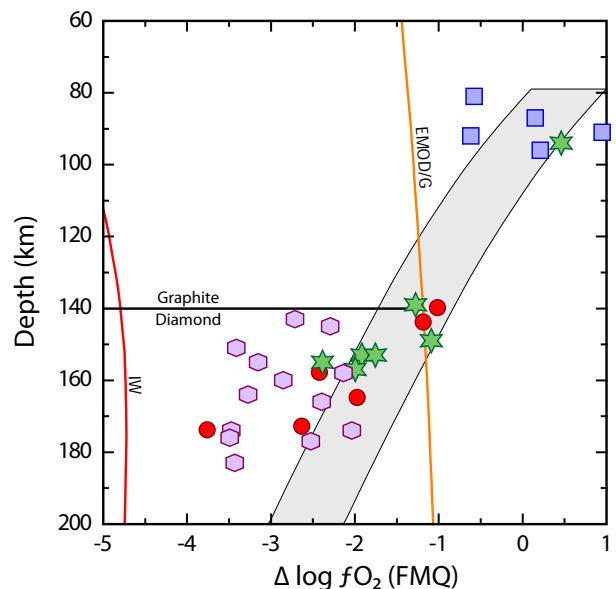


Figure 4. Depth versus  $\Delta \log fO_2$  (FMQ) for Diavik xenoliths. The enstatite – magnesite – olivine – diamond / graphite (EMOD/G), iron-wüstite (IW) and diamond-graphite reaction boundaries are shown for reference. The shaded area indicates the “pre-metasomatic” redox profile for the central Slave lithospheric mantle calculated along a 41 mW/m<sup>2</sup> reference geotherm taking the least metasomatized samples as the starting point. The more intensely metasomatized deeper samples fall to the low- $fO_2$  side of this profile indicating that re-enrichment of the lower portion of the Slave lithospheric mantle was connected with reduction and hence diamond friendly. Symbols are the same as in Figure 3.

---

## References

- Aulbach S, Griffin WL, Pearson NJ, O'Reilly SY, Doyle BJ (2007) *Contrib Mineral Petrol* 154:409-427
- Brey GP, Köhler T (1990) *J Petrol* 31:1353-1378
- Creighton S, Stachel T, Matveev S, Höfer H, McCammon C, Luth RW (2008) *Contrib. Mineral Petrol* (Submitted)
- Griffin WL, Doyle BJ, Ryan CG, Pearson NJ, O'Reilly SY, Davies R, Kivi K, Van Achterbergh E, Natapov LM (1999) *J Petrol* 40:705-727
- Grütter HS, Gurney JJ, Menzies AH, Winter F (2004) *Lithos* 77:841-857
- Gudmundsson G, Wood BJ (1995) *Contrib Mineral Petrol* 119:56-67
- Höfer HE, Brey GP (2007) *Am Min* 92:873-885
- Menzies A, Westerlund K, Grütter H, Gurney J, Carlson J, Fung A, Nowicki T (2004) *Lithos* 77:395-412
- O'Neill HSC, Wood BJ (1979) *Contrib Mineral Petrol* 70:59-70
- Pearson NJ, Griffin WL, Doyle BJ, O'Reilly SY, van Achterbergh E, Kivi K (1999) *Proc. VII<sup>th</sup> International Kim. Conf.* pp 109-116